

## ARTICLES

### Dissociation of Methane in Intense Laser Fields

Sufan Wang, Xiaoping Tang, Lirong Gao, Mohamed E. Elshakre,<sup>†</sup> and Fanao Kong\*

*Institute of Chemistry, Chinese Academy of Science, Beijing 100080, China*

*Received: October 16, 2002; In Final Form: May 15, 2003*

The dissociation of methane in the intense laser field has been investigated experimentally and theoretically. Using an amplified ultrafast Ti:sapphire laser around 800 nm coupled to a TOF mass spectrometer, all the primary and secondary ions were produced and detected at the laser intensities  $10^{13}$  to  $10^{14}$  W/cm<sup>2</sup>. The experimental results show that the dissociation of methane proceeds via a stepwise mechanism by gradually increasing the laser intensity. The maximum H<sup>+</sup> yield is formed when the linearly polarized laser field is parallel to the axis of the TOF tube. A quasi-diatom theoretical model has been proposed and used to interpret the dissociation of polyatomic molecules. The model assumes that only the dissociative bond is considered and the rest of the molecular geometry is fixed during the dissociation. For each step, the profiles of the dressed potential energy surfaces (PESs) along the dissociative bond of the molecule at different laser intensities are calculated. Quasi-classical trajectories on the dressed PESs are calculated, showing that the wave packet is modulated by the sinusoidal laser field. Theoretical dissociation probabilities are thus calculated. The results can fully interpret the overall dissociation processes and the angular dependence of H<sup>+</sup> yield.

#### I. Introduction

A strong electric field can make large changes in the properties of molecules. Once the field intensity attains  $10^8$  V/cm, the typical strength felt by the valence electrons, the molecules ionize and dissociate in a process called field ionization (FI) and field dissociation (FD). Modern ultrafast lasers provide field intensities that exceed the intramolecular field strengths. For the wavelength 800 nm, the electric field amplitude in a laser beam is given by  $E = 27.4(I)^{1/2}$ , where  $I$  is the peak intensity expressed in watts per square centimeter, while  $E$  is in volts per centimeter.

At an intense laser field of  $10^{13}$  to  $10^{14}$  W/cm<sup>2</sup>, chemical bonds can be broken in all types of molecules even within a single laser shot. Obviously, the dissociation mechanism is different from that of multiphoton dissociation (MPD) with a

weaker laser intensity ( $> 10^9$  W/cm<sup>2</sup>). MPD has a strong laser wavelength dependence and usually breaks one bond in the excited state of a molecule.

A widely accepted dissociation mechanism is Coulomb explosion, which is the fragmentation of a doubly or multiply charged molecule driven by the intramolecular Coulomb repulsive force. The Coulomb explosion explains why small fragments result from excitation by an ultrafast laser pulse. The charge-resonance-enhanced ionization (CREI) theory suggests that, at the beginning of the laser-molecule interaction, the dissociation of H<sub>2</sub><sup>+</sup> into H + H<sup>+</sup> is a dominant process.<sup>1</sup> A model used to explain dissociation of strongly bound diatomic molecules was proposed by Corkum.<sup>2</sup> Many studies have been performed on the dissociative ionization of diatomic and triatomic molecules.<sup>3–14</sup>

A few studies had been reported by Cornaggia,<sup>3–5,15</sup> Mathur,<sup>16–19</sup> Castillejo,<sup>20,21</sup> Ledingham,<sup>22–26</sup> and Wu<sup>27</sup> on the dynamical behavior of polyatomic molecules. For polyatomic molecules it is difficult to explain the fragmentation following

\* To whom correspondence should be addressed. Telephone: 86-10-62555347. Fax: 86-10-62563167. E-mail: kong@mrmlab.icas.ac.cn.

<sup>†</sup> Permanent address: Chemistry Department, College of Science, Cairo University, Cairo, Egypt.

a Coulomb explosion. When the molecular size increases, the intramolecular Coulomb repulsive force becomes weaker. However, extensive fragmentation of some large molecules has been observed even at  $10^{13}$  W/cm<sup>2</sup>.<sup>28</sup> Furthermore, only the singly charged ions are formed at the laser intensity. The fact cannot be interpreted by a Coulomb explosion mechanism, which presupposes forming multiply charged molecular ions. Therefore, a new mechanism for the field dissociation of polyatomic molecules is invoked. Mathur et al. tried to interpret the dissociation based on the changes in the electron charge distribution.<sup>29</sup> Recently, Lezius et al.<sup>30</sup> proposed a multielectron excitation–ionization mechanism in another attempt to solve the puzzle.

In this work, we intend to understand the field dissociation of polyatomic molecules from a new point of view; that is, the laser field takes the molecule apart simply by pulling off a chemical bond, whose axis is along the field vector. The bond-rupture can take place even in a singly charged molecular ion at relative low laser intensity. To check the validity of such a hypothesis, a study is carried out at the laser intensity  $10^{13}$  to  $10^{14}$  W/cm<sup>2</sup> in both experimental and theoretical aspects. We have found some evidences supporting the new viewpoint. The evidences show that the field dissociation of a polyatomic molecule consists of a sequence of individual dissociation steps. Only the singly charged fragment ions are found in the mass spectrum at the laser intensity. Using a linearly polarized laser technique, we verify that the dissociation takes place along the laser field vector. From the theoretical aspect, we propose a simple field dissociation model. With this model, not only can the stepwise dissociation processes be reasonably interpreted but also the dissociation probability, the threshold field intensity, and the dissociation time of the molecular ion can be quantitatively calculated. The calculated results agree with the experimental observations.

In a previous paper, we reported that we have successfully used the primary theory of this model to explain the stepwise dissociation of acetone in an intense laser field.<sup>31</sup> However, comprehensive description and calculating procedures of the theory have not been mentioned. Here we report a study on the dissociation of another polyatomic molecule, methane, in an intense laser field. Not only has a careful experimental investigation been performed but also a detailed description of the model and its calculation procedures are presented.

There are a number of studies focused on the interaction of intense laser fields with methane. Cornaggia has studied the dissociation of methane,<sup>32</sup> and their results were interpreted on the basis of multielectron dissociative ionization in the very high-intensity regime  $10^{15}$  to  $10^{16}$  W/cm<sup>2</sup>, where the production of multicharged ions is observed. They were able to detect the parent ion and all the fragment species including the multiply charged atomic species. In contrast, Mathur and co-workers studied the dissociation of methane<sup>33</sup> using long laser pulses (35 ps) and at an intensity of  $10^{14}$  W/cm<sup>2</sup>. They had surprisingly different dissociation products, where they detected the parent ion and all the secondary dissociation products, with no sign of the production of the primary fragment, CH<sub>3</sub><sup>+</sup> ion. They interpreted the absence of the CH<sub>3</sub><sup>+</sup> in terms of charge migration, upon subjecting methane to the intense laser field, resulting in the instability of the CH<sub>3</sub><sup>+</sup> fragment. Very recently, Wu and co-workers<sup>34</sup> studied the laser-induced dissociation and explosion of methane in the intensity range  $6 \times 10^{13}$  to  $3 \times 10^{15}$  W/cm<sup>2</sup> using 110 fs laser pulses. They interpreted their results in terms of Coulomb explosion based on the detection of highly charged atomic ions. Neither of these reports addressed the

stepwise nature of the dissociation of methane in intense laser fields. It was our objective to investigate the dissociation of methane in intense laser fields from a new point of view, which considers that the laser field directly breaks the chemical bonds.

## II. Experimental Section

The laser system used in this experiment was a home-built mode-locked femtosecond Ti:sapphire oscillator, which was pumped by a diode-pumped, frequency-doubled laser (532 nm, Coherent, Verdi). As a seed pulse, the 800 nm, 30 fs laser pulse from the oscillator was stretched and then led to a multipass Ti:sapphire laser amplifier (Quantronix, Odin) which was pumped by the second harmonic of a Nd:YLF laser. The amplified laser beam was compressed to 160 fs, and the maximum energy output was about 300  $\mu$ J per pulse. The beam divergence was  $0.25 \pm 0.02$  mrad. The amplified femtosecond pulse was focused into the chamber of the linear TOF mass spectrometer by a 15 cm focal lens. The gaseous molecules were continuously effused into the chamber through an orifice with an i.d. of 500  $\mu$ m. A background pressure of  $1.9 \times 10^{-6}$  Torr and a pressure of methane gas of  $3.4 \times 10^{-6}$  Torr were maintained. The fragment ions produced in the laser beam were extracted by 200 V and then accelerated by 900 V in a two-stage electric field and fly freely to a dual microchannel plate (MCP) through a 50 cm free-field flight tube. The ion signal was detected by the MCP and acquired by a 100 MHz high-speed transient recorder and then transferred to the computer for data acquisition.

For the laser polarization experiment, the extraction voltage was set to zero and the ions produced in the laser beam moved just through a 3 mm diameter hole to the acceleration region. The distance between the hole and the laser interaction region was 8 mm. Only those ions whose divergence referred to the TOF axis was less than 11° can reach the MCP. A  $\lambda/2$  wave-plate was inserted into the path of the laser beam before the window of the chamber. A polarizer was used to determine the initial angle of the  $\lambda/2$  wave-plate. The mass spectrum can be obtained at different laser polarizations by rotating the  $\lambda/2$  wave-plate.

## III. Model and Calculations

Since ionization of polyatomic molecules usually takes place at lower laser intensity ( $10^{13}$  W/cm<sup>2</sup>), we will consider the dissociation of molecular ions rather than that of the neutral molecule. When a laser field is applied to a molecular ion, only ions having a bond that is parallel to the laser electric field vector are taken into consideration. Our model assumes that in the strong field only the bond length, which lies along the laser field, changes while the rest of the molecular geometry is fixed. The model also assumes that only the ground electronic state of the dissociative molecular ion is considered. We will prove that, in a sufficiently strong laser field, polyatomic molecules spontaneously dissociate due to the stretching of their chemical bonds. The model can be called a field-assisted dissociation (FAD) model. The application of the model to the dissociating process in an intense field thus consists of the following calculating procedures: the dressed potential energy surfaces (PESs) of the ground state of the molecular ion at different field intensities; quasi-classical trajectory (QCT) calculations for the bond lengths with time; the average dissociation time; and the dissociation probability.

**A. PES Calculations.** The calculation starts with optimizing the geometry of the neutral molecule and the molecular ion. The dissociative bond is assumed to be set parallel to the electric

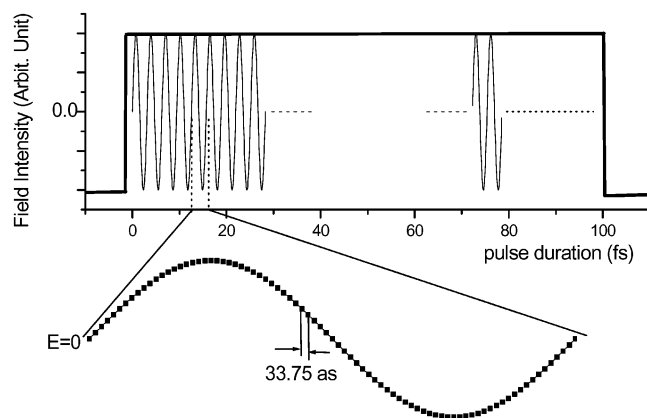


**Figure 1.** Rectangular envelope of the 100 fs laser pulse divided into 37 sinusoidal optical cycles. Each cycle has a time duration of 2.7 fs. In the calculation, each cycle consists of 80 steps.

field vector of the applied laser. The ground-state PESs along the dissociation bond have been calculated at different field intensities, in the level of Hartree-Fock (RHF or UHF)/6-31G with the “FIELD” option in the Gaussian 98 package.<sup>35</sup> This is done at different field intensities and with two opposite directions of the electric field along the dissociative bond axis, since the optical oscillating field changes its direction alternatively and periodically. All the dressed PESs are distorted by the applied electric field, especially on the large bond distance side. The field intensities used in the calculation are  $<0.2$  au, where the perturbation theory can be considered valid.

**B. Quasi-classical Trajectory Calculations.** The dissociation dynamics of the molecular ion can be considered as the bond being stretched by the laser field. The nuclear motion can be thus represented by a motion of the Gaussian wave packet and assumed to take place on a ground dressed PES, which is modulated by the oscillating laser field. The driving force is proportional to the slope of the dressed PES at the corresponding distance.

We consider a Gaussian wave packet in the Wigner representation moving on and across the PESs. This wave packet motion starts from the field-free PES and periodically goes through various dressed PESs at different laser intensities, executing horizontal motion along the PES and then vertically to the next PES.

At that point, we consider the optical field of the 100 fs laser pulse duration. Such a field can be considered as a monochromatic field with slow amplitude modulation and causing a sinusoidal perturbation to the two rigid fragments. Provided with the experimental value of the laser wavelength 800 nm, the width of an optical cycle is 2.7 fs. The laser pulse can be thought of as having an envelope of rectangular shape; we can find that, within the 100 fs pulse, there are  $100/2.7 = 37$  cycles (Figure 1). To make sure that the time is much shorter than one vibrational period, we divide the 2.7 fs pulse into 80 slots in the following calculations. Each slot will represent a time of  $2.7/80 = 33.75$  attoseconds (as) or 0.03375 fs. That is the time used by the wave packet to execute its motion along a PES and across to the next PES. The QCT calculations start at a value of  $R_0$ , which is equal to the equilibrium bond distance of the neutral molecule, where we are assuming that during the extremely rapid ionization process the molecular geometry does not change. It is also assumed that the initial velocity  $v_0$  of the wave packet is zero. The wave packet starts moving along the field-free PES of the molecular ion for 33.75 as, followed by sliding vertically downward to the first dressed ground-state PES at the lowest applied laser intensity, and so on. The evolution

of the trajectory of the wave packet in the modulated field can be visualized when we imagine its motion in one optical cycle. In the first half of the optical cycle, the wave packet moves across and along all the 40 PESs, with the electric field parallel to the dissociating bond in one direction. The wave packet starts to move from the field-free PES to the highest dressed PES and back again to the field-free PES. In the second half of the optical cycle, the wave packet executes the same type of motion as in the first half, but with the electric field pointing in the opposite direction. Then, the motion of the wave packet is repeated for the entire pulse duration of 100 fs.

Thousands of the trajectories reflect the change of the dissociating bond with time. The change of the dissociating bond with time is obtained by averaging these trajectories. It will be shown later that the dissociative bond is modulated by the field. Under a moderate field intensity, the bond distance oscillates with time. For strong fields the bond distance monotonically increases. A threshold laser intensity can be defined by the intensity that causes 1% dissociation in the weighted trajectories. We have assumed 6 Å to be the distance for which the bond can be considered broken.

The dissociation probability can also be defined as the ratio of the weighted number of the dissociative trajectories leading to the total number of trajectories.

#### IV. Results and Discussion

**A. Primary Dissociation Channel.** We detected the dissociation products as a function of increasing laser intensity. The dissociation patterns reveal a stepwise dissociation feature. Figure 2a shows, at the intensity  $7.6 \times 10^{13}$  W/cm<sup>2</sup>, a peak of 16 atomic mass units (amu), corresponding to the parent ion CH<sub>4</sub><sup>+</sup>. This indicates that only the neutral CH<sub>4</sub> undergoes ionization.

By slightly increasing the laser intensity to  $8.0 \times 10^{13}$  W/cm<sup>2</sup>, the mass spectrum recorded three peaks corresponding to the parent ion, CH<sub>4</sub><sup>+</sup> (16 amu), the primary fragment ions, CH<sub>3</sub><sup>+</sup> (15 amu), and H<sup>+</sup> (1 amu). Figure 2b clearly indicates the dissociation of one of the four equivalent C–H bonds at that particular laser intensity.

The FAD model is applied to calculate the primary dissociation process of CH<sub>4</sub><sup>+</sup> ion. A potential well of 28.1 kcal/mol along the C–H bond in the zero-field PES of the ground state of the CH<sub>4</sub><sup>+</sup> ion is found in our calculation. The PES is distorted by the laser field at different field intensities, as shown in Figure 3. The QCT calculated results predict that the H<sup>+</sup> ion can be pulled from the parent ion CH<sub>4</sub><sup>+</sup> even for the laser intensity as low as  $5.6 \times 10^{13}$  W/cm<sup>2</sup>. The FAD model can also interpret the electric charge distribution in the dissociation process or predict the preference of the reaction channel



or

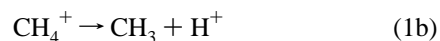
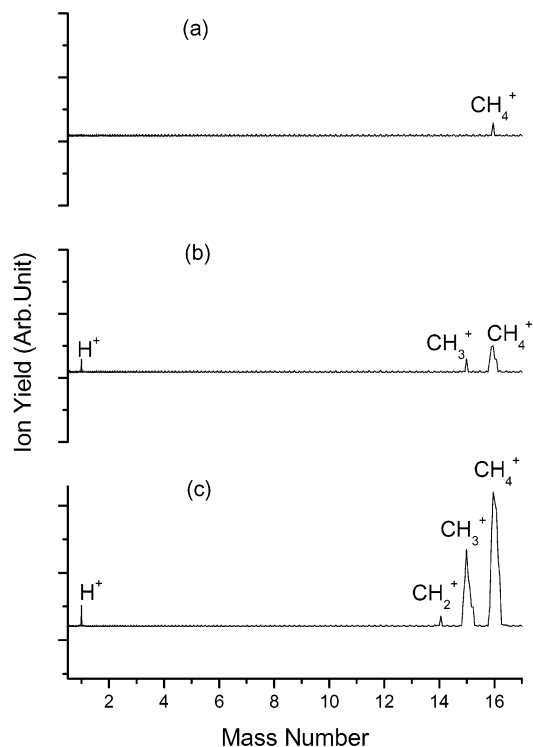


Figure 3 shows the effects of both the field direction and the field intensity on the shape of the PESs. When the electric field vector is directed toward the H atom, as represented by Figure 3a, the PES is more affected and suffering more distortion, implying higher tendency for dissociation. The dissociation channel (reaction 1b) yielding a primary fragment ion H<sup>+</sup> and CH<sub>3</sub> is thus the favored channel. On the contrary, Figure 3b shows that the PES is less affected and less distorted by the

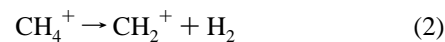


**Figure 2.** TOF mass spectrum of methane irradiated by an intense laser (160 fs laser pulses at 800 nm) at the laser intensity of (a)  $7.6 \times 10^{13}$  W/cm<sup>2</sup>, (b)  $8.0 \times 10^{13}$  W/cm<sup>2</sup>, or (c)  $1.0 \times 10^{14}$  W/cm<sup>2</sup>.

electric field vector, reflecting less tendency of dissociation. As a result, for the more unstable CH<sub>4</sub><sup>+</sup> ion, its electronic charge distribution shifts to the CH<sub>3</sub> group but not to the H atom. In other words, reaction 1b is the preferable channel. The evidence of such a preference can be found in the angular distribution experiment, which will be described in the latter part of this article.

**B. Secondary Dissociation Channels. Production of the CH<sub>2</sub><sup>+</sup> Ion.** When the laser intensity is increased, the primary fragment ion, CH<sub>3</sub><sup>+</sup>, undergoes sequential dissociation into smaller fragment ions. Figure 5 shows that as the laser intensity increases to  $1.0 \times 10^{14}$  W/cm<sup>2</sup>, the peak at 14 amu appears, corresponding to the production of CH<sub>2</sub><sup>+</sup>. CH<sub>2</sub><sup>+</sup> ion can possibly

result from two possible dissociation channels, namely

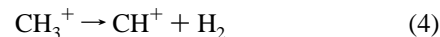


or



The dissociation probability of the channel in eq 2 can be obtained by assuming that the laser field vector exerts on the T<sub>d</sub> axis of the CH<sub>4</sub><sup>+</sup> molecular ion. If some of the CH<sub>3</sub><sup>+</sup> ions rotate in the same laser pulse and one of their C–H bonds aligns along the field vector, the dissociation probability of the channel in eq 3 can also be calculated. The calculations show that the dissociation channel in eq 3 is the main dissociation channel for CH<sub>2</sub><sup>+</sup> production, since the calculated dissociation probability for channel 3 is 99.9% and that of channel 2 is only 4.8% at the laser intensity of  $7.9 \times 10^{14}$  W/cm<sup>2</sup>. The calculated trajectory of the averaged H–CH<sub>2</sub><sup>+</sup> distance is shown in Figure 4. The bond distance has been elongated to 6 Å within 40 fs at  $7.9 \times 10^{14}$  W/cm<sup>2</sup>. Another proof for considering channel 3 as the sole channel for the production of the CH<sub>2</sub><sup>+</sup> comes from the inspection of the mass spectra of Figure 2c, where there is no evidence for the production of H<sub>2</sub><sup>+</sup> ion produced through channel 2. H<sub>2</sub><sup>+</sup> ion appears only at higher laser intensities, as evidenced from Figure 5. To verify this further, we have investigated the dissociation of methyl-containing molecules such as acetaldehyde and acetone. We found that the CH<sub>3</sub><sup>+</sup> → CH<sub>2</sub><sup>+</sup> + H occurs almost at the same laser intensity as that shown in the inset of Figure 5.

**Production of CH<sup>+</sup> and C<sup>+</sup>.** Upon increasing the laser intensity to  $1.3 \times 10^{14}$  W/cm<sup>2</sup>, several additional peaks appear at 13 and 12 amu, corresponding to the production of CH<sup>+</sup> and C<sup>+</sup>, respectively, as shown in Figure 5. There are two possible channels for the production of CH<sup>+</sup> fragment ion.



To distinguish which channel is responsible for the production of the secondary ion CH<sup>+</sup>, both the distortions of the PES of the precursor ions CH<sub>3</sub><sup>+</sup> and CH<sub>2</sub><sup>+</sup> are inspected. These are

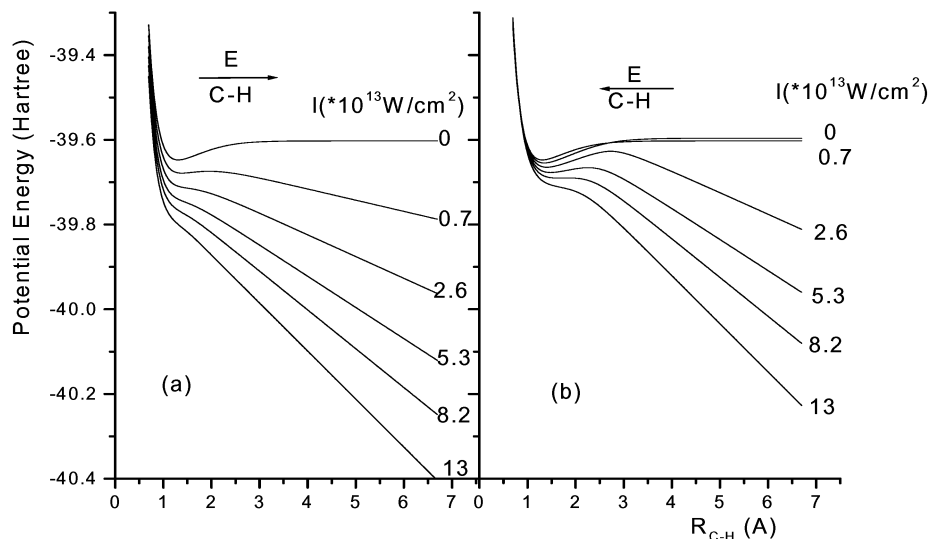


**Figure 3.** Potential energy surfaces (PESs) of the CH<sub>4</sub><sup>+</sup> at different laser intensities and in two opposite laser field directions. The field vector is shown by the arrows: (a) C → H; (b) C ← H.

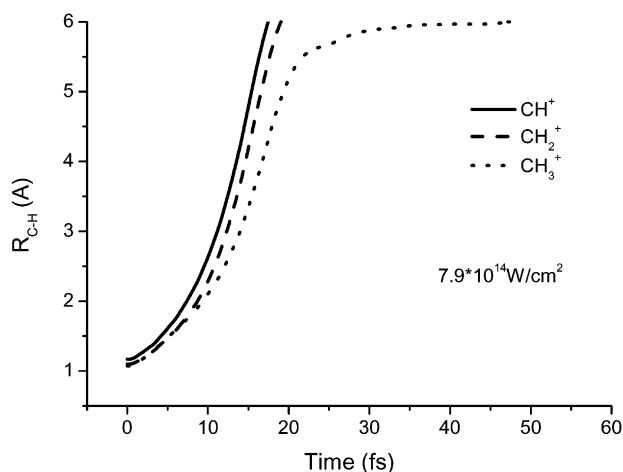


**Figure 4.** Quasi-classical trajectory of the averaged C–H distances of  $\text{CH}^+$ ,  $\text{CH}_2^+$ , and  $\text{CH}_3^+$  ions at the laser intensity of the field ( $I = 7.9 \times 10^{14} \text{ W/cm}^2$ ).

shown in Figures 6 and 7, respectively. The comparison shows that the distortion of the PES of the  $\text{CH}_2^+$ , with the field in both directions represented by Figure 7, is more serious than that of the PES of the  $\text{CH}_3^+$ , shown in Figure 6. Hence, the higher tendency of  $\text{CH}_2^+$  dissociation indicates that dissociation channel 5 is preferentially responsible for the production of the  $\text{CH}^+$  ions. QCT calculations on the production of  $\text{CH}^+$  via both the dissociation channels 4 and 5 have been performed. The dissociation probability at an intensity of  $7.9 \times 10^{14} \text{ W/cm}^2$  was found to be less than 0.001% for channel 4 and 100% for channel 5, indicating that the  $\text{CH}^+$  is produced from  $\text{CH}_2^+$  ion (Figure 4).

Likewise, and based on similar calculations, we conclude that  $\text{C}^+$  is produced from the dissociation of the  $\text{CH}^+$  ions



The QCT result of the  $\text{C}^+$ –H bond distance is also shown in Figure 4. The theoretical dissociation threshold of the  $\text{CH}_3^+$  dissociating to  $\text{CH}_2^+$  was  $3.5 \times 10^{14} \text{ W/cm}^2$ , while that of the  $\text{CH}_2^+$  dissociating to  $\text{CH}^+$  and that of the  $\text{CH}^+$  dissociating to  $\text{C}^+$  are the same intensity,  $2.9 \times 10^{14} \text{ W/cm}^2$ .

The comparison between the dissociation thresholds of the three ions clearly indicates that the  $\text{CH}_3^+$  ions have the highest dissociation thresholds.  $\text{CH}_2^+$  formation acts as a bottleneck step for the formation of the  $\text{CH}^+$  and  $\text{C}^+$  ions. This is the reason  $\text{CH}_2^+$ ,  $\text{CH}^+$ , and  $\text{C}^+$  appear at the same laser intensity. Similar observations have been obtained for  $\text{CH}_3$ -containing compounds and shown in the inset of Figure 5.

**C. Angular Distribution of the Fragment Ions.** The angular distribution of the fragment ions was detected using a linearly polarized laser beam. At the laser intensity  $1.8 \times 10^{14} \text{ W/cm}^2$ , the maximum yield of  $\text{H}^+$  ions was found when the laser polarization vector was parallel to the axis of the TOF mass spectrometer, while the minimum yield was recorded when the laser polarization vector was perpendicular (Figure 8). On the contrary, other ions  $\text{CH}_3^+$ ,  $\text{CH}_2^+$ ,  $\text{CH}^+$ , and  $\text{C}^+$  did not exhibit such angular dependence. Methane is a molecule without a permanent dipole, so that dynamic alignment may not have a contribution to the angular dependence of the dissociating ions. The only reasonable interpretation of such a dependence is that the laser field coincides with one of the C–H bonds of the  $\text{CH}_4$  molecule. The strong field causes the bond to break, driving the  $\text{H}^+$  ion as a primary product away along the field vector. In

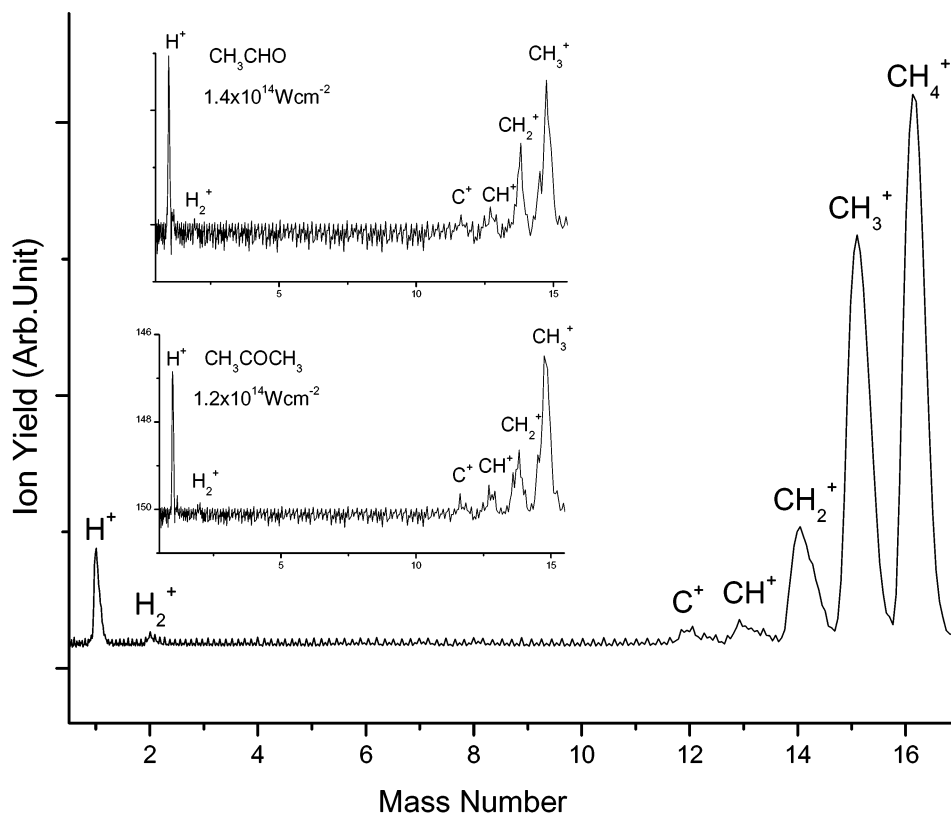


**Figure 5.** TOF mass spectrum of methane irradiated by a 160 fs, 800 nm laser at the intensity  $1.3 \times 10^{14} \text{ W/cm}^2$ . The inset shows the mass spectra of  $\text{CH}_3\text{CHO}$  and  $\text{CH}_3\text{COCH}_3$ , verifying the similarity of the dissociation thresholds and dissociation profile of the  $\text{CH}_3^+$  ion into the secondary fragments  $\text{CH}_2^+$ ,  $\text{CH}^+$ , and  $\text{C}^+$ , among the  $\text{CH}_3$ -carrying molecules.

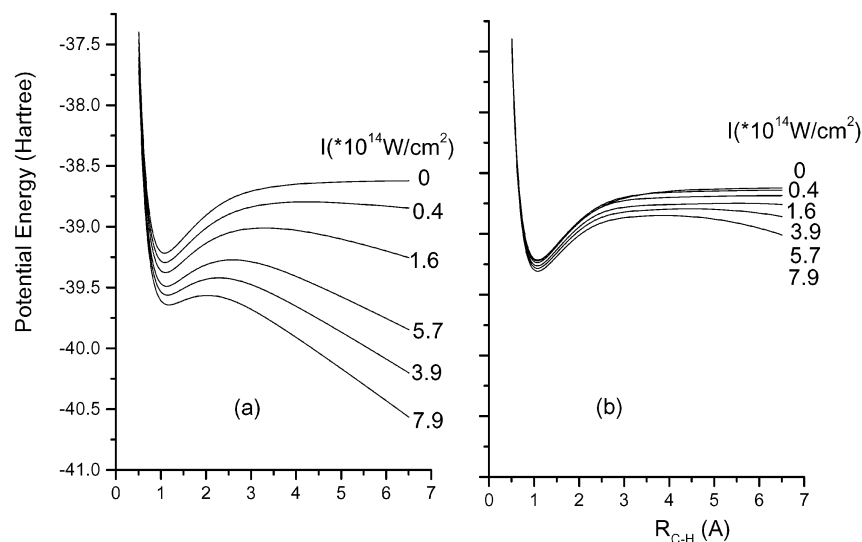


**Figure 6.** Potential energy surfaces (PESs) of the  $\text{CH}_3^+$  at different laser intensities and in two opposite laser field directions. The field vector is shown by the arrows: (a)  $C \rightarrow H$ ; (b)  $C \leftarrow H$ .

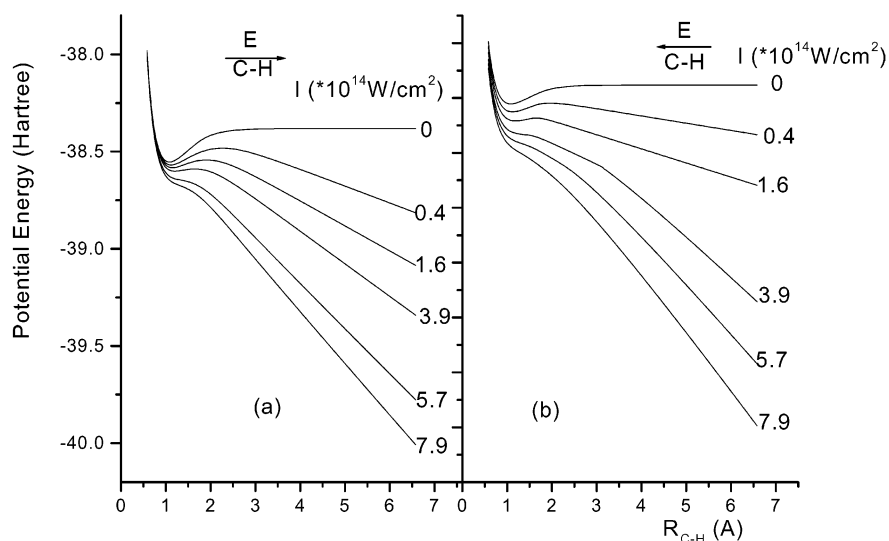


**Figure 7.** Potential energy surfaces (PESs) of the  $\text{CH}_2^+$  at different laser intensities and in two opposite laser field directions. The field vector is shown by the arrows: (a)  $C \rightarrow H$ ; (b)  $C \leftarrow H$ .

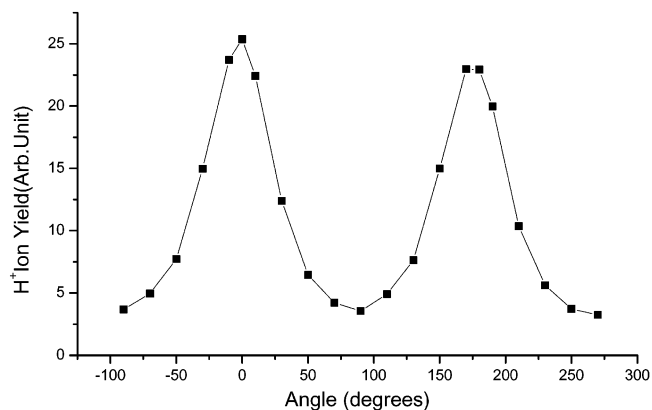


**Figure 8.** Dependence of the  $\text{H}^+$  yield on the angle between the laser polarized plane and the TOF axis. The field intensity is  $1.8 \times 10^{14} \text{ W/cm}^2$ .

other words, the theoretically predicted preferable reaction channel 1b has been identified by this experimental result.

## V. Concluding Remarks

The stepwise dissociation of methane in the  $10^{13}$  to  $10^{14} \text{ W/cm}^2$  intensity regime from 800 nm and 100 fs laser pulses has been verified by gradually increasing the laser intensity and monitoring the dissociation products using TOF MS. The parent ion,  $\text{CH}_4^+$ , was obtained at the lowest laser intensity,  $7.6 \times 10^{13} \text{ W/cm}^2$ . The primary fragment ion,  $\text{CH}_3^+$ , appeared at  $8.0 \times 10^{13} \text{ W/cm}^2$ . The secondary fragment ions  $\text{CH}_2^+$ ,  $\text{CH}^+$ , and  $\text{C}^+$  were obtained at the laser intensities  $1.0 \times 10^{14}$ ,  $1.3 \times 10^{14}$ , and  $1.3 \times 10^{14} \text{ W/cm}^2$ , respectively. The  $\text{CH}^+$  ion was produced by breaking one of the  $\text{C-H}$  bonds of  $\text{CH}_2^+$ . The  $\text{H}^+$  fragments show a strong angular dependence. This has been interpreted as the laser field breaking the  $\text{C-H}$  bond and pulling the  $\text{H}^+$  apart along the field vector.

A so-called FAD model has been proposed on the basis of the assumption that, during dissociation, only the dissociative bond is taken into account and the rest of the molecular geometry is fixed. The dressed PESs are modulated by the laser field at different laser intensities and two opposite electric field

directions. QCT calculations can be performed for the bond-breaking process. The wave packet moves on a series of dressed PESs that change with the external field. The calculations provide values for the dissociation threshold intensities and probabilities. The FAD mechanism successfully interprets the entire dissociation process. Two shortcomings of the model are the assumptions that only one bond is being considered during the dissociation process and that only the ground state PES is considered for calculations. The theoretical model used in this work is certainly a simple one, but the agreement with experiment is good. Such agreement gains an insight into the essence of the dissociation of molecules in an intense laser field. Furthermore, this study is also relevant to laser control in an intense laser field, which has been reported recently.<sup>36,37</sup> According to this model, the dissociation of molecular ions may be controlled by regulating the laser peak intensity and the pulse duration. For laser control involving quantum interference, this model can also shed light on the nuclear motion of the molecular ion being controlled.

**Acknowledgment.** This work is supported by the NKBRFSF project and CNSF under Contract Number 29973052. The authors would like to thank Dr. Jishu Shao for his help with QCT calculations, Dr. Hongfei Wang and Andong Xia for their technical assistance with the laser system, and the national supercomputing center of China, Beijing, for the allocated computer time. One of us, ME, is indebted to the research fellowship from the Third World Academy of Science, TWAS, to conduct this research project.

## References and Notes

- (1) Chelkowsky, S.; Conjusteau, A.; Zuo, T.; Bandrauk, A. D. *Phys. Rev. A* **1996**, *54* (4), 3235.
- (2) Dietrich, P.; Corkum, P. J. *Chem. Phys.* **1992**, *97* (5), 3187.
- (3) Cornaggia, C.; Herring, Ph. *Phys. Rev. A* **2000**, *62*, 023403.1–023403.13.
- (4) Hering, Ph.; Cornaggia, C. *Phys. Rev. A* **1998**, *57* (6), 4572–4580.
- (5) Cornaggia, C.; Normand, D.; Morellec, J. J. *Phys. B: At., Mol. Opt. Phys.* **1992**, *25*, L415–L422.
- (6) Kumar, G. R.; Safvan, C. P.; Rajgara, F. A.; Mathur, D. *J. Phys. B: At., Mol. Opt. Phys.* **1994**, *27*, 2981–2991.
- (7) Cornaggia, C.; Schmidt, M.; Normand, D. *J. Phys. B: At., Mol. Opt. Phys.* **1994**, *27*, L123–L130.
- (8) Cornaggia, C.; Solin, F.; Leblanc, C. *J. Phys. B: At., Mol. Opt. Phys.* **1996**, *29*, L749–L754.
- (9) Safvan, C. P.; Thomas, R. V.; Mathur, D. *Chem. Phys. Lett.* **1998**, *286*, 329–335.
- (10) Safvan, C. P.; Bhardwaj, V. R.; Kumar, G.; Mathur, D.; Rajgara, F. A. *J. Phys. B: At., Mol. Opt. Phys.* **1996**, *29*, 3135–3149.
- (11) Banerjee, V. R.; Kumar, G. R.; Mathur, D. *J. Phys. B: At., Mol. Opt. Phys.* **1999**, *32*, 4277–4292.
- (12) Bhardwaj, V. R.; Vijayalakshmi, K.; Rajgara, F. A.; Mathur, D. *J. Phys. B: At., Mol. Opt. Phys.* **1999**, *32*, 1087–1095.
- (13) Banerjee, S.; Kumar, G. R.; Mathur, D. *Phys. Rev. A* **1999**, *60* (5), R3369–R3372.
- (14) Safvan, C. P.; Vijayalakshmi, K.; Rajgara, F. A.; Kumar, G. R.; Mathur, D. *J. Phys. B: At., Mol. Opt. Phys.* **1996**, *29*, L481–L487.
- (15) Cornaggia, C. *Phys. Rev. A* **1995**, *52*, R4328–R4331.
- (16) Mathur, D.; Safvan, C. P.; Kumar, G. R.; Krishnamurthy, M. *Phys. Rev. A* **1994**, *50*, R7–R9.
- (17) Bhardwaj, V. R.; Vijayalakshmi, K.; Mathur, D. *Phys. Rev. A* **1999**, *59* (2), 1392–1398.
- (18) Vijayalakshmi, K.; Bhardwaj, V. R.; Mathur, D. *J. Phys. B: At., Mol. Opt. Phys.* **1997**, *30*, 4065–4085.
- (19) Bhardwaj, V. R.; Vijayalakshmi, K.; Mathur, D. *Phys. Rev. A* **1997**, *56* (3), 2455–2458.
- (20) Castillejo, M.; Couris, S.; Koudomas, E.; Martin, M. *Chem. Phys. Lett.* **1999**, *308*, 373–380.
- (21) Castillejo, M.; Couris, S.; Koudomas, E.; Martin, M. *Chem. Phys. Lett.* **1998**, *289*, 303–310.
- (22) Ledingham, K. W.; Singhal, R. P.; Smith, D. J.; McCanny, T.; Graham, P.; Kilic, H. S.; Peng, W. X.; Wang, L. S.; Langley, A. J.; Taday, P. F. *J. Phys. Chem. A* **1998**, *102*, 3002–3005.
- (23) Smith, D. J.; Ledingham, K. W. D.; Kilic, H. S.; McCanny, T.; Peng, W. X.; Singhal, R. P.; Langley, A. J.; Taday, P. F.; Kosmidis, C. *J. Phys. Chem. A* **1998**, *102*, 2519–2526.
- (24) Kosmidis, C.; Ledingham, K. W.; Kilic, H. S.; McCanny, T.; Singhal, R. P.; Langley, A. J.; Shaikh, W. *J. Phys. Chem. A* **1997**, *101*, 2264–2270.
- (25) Tzallas, P.; Kosmidis, C.; Ledingham, K. W. D.; Singhal, R. P.; McCanny, T.; Graham, P.; Hankin, S. M.; Taday, P. F.; Langley, A. J. *J. Phys. Chem. A* **2001**, *105*, 529–536.
- (26) Ledingham, K. W. D.; Ledingham, R. P. S. *Int. J. Mass Spectrom. Ion Processes* **1997**, *163*, 149–168.
- (27) Wu, C. Y.; Ren, H. Z.; Liu, T. T.; Ma, R.; Yang, H.; Hongling, J.; Gong, Q. H. *J. Phys. B: At., Mol. Opt. Phys.* **2002**, *35*, 1–8.
- (28) Wu, C.; Xiong, Y.; Ji, N.; He, Y.; Gao, Z.; Kong, F. *J. Phys. Chem. A* **2001**, *105*, 374–377.
- (29) Vijayalakshmi, K.; Bhardwaj, V. R.; Mathur, D. *J. Phys. B: At., Mol. Opt. Phys.* **1997**, *30*, 4065–4085.
- (30) Lezius; et al. *Phys. Rev. Lett.* **2001**, *86* (1), 51.
- (31) Tang, X.; Wang, S.; Elshakre, M. E.; Gao, L.; Wang, Y.; Wang, H.; Kong, F. *J. Phys. Chem. A* **2003**, *107* (1), 13.
- (32) Hering, Ph.; Cornaggia, C. *Phys. Rev. A* **1998**, *57* (6), 4572–4580.
- (33) Mathur, D.; Safvan, C. P.; Kumar, G. R.; Krishnamurthy, M. *Phys. Rev. A* **1994**, *50* (1), R7–R9.
- (34) Wu, C.; Ren, H.; Liu, T.; Ma, R.; Yang, H.; Jiang, H.; Gong, Q. *J. Phys. B: At., Mol. Opt. Phys.* **2002**, *35*, 1–8.
- (35) Frisch, M. J.; et al. *Gaussian 98*, Revision A.7; Gaussian Inc.: Pittsburgh, PA, 1998.
- (36) Assion, A.; Baumert, T.; Bergt, M.; Brixner, T.; Kiefer, B.; Seyfried, V.; Strehle, M.; Gerber, G. *Science* **1998**, *282*, 919.
- (37) Levis, R. J.; Menkir, G. M.; Rabitz, H. *Science* **2001**, *292*, 709–713.